

Tunneling and propagation of vacuum bubbles on dynamical backgrounds

Dennis Simon¹, Julian Adamek¹, Aleksandar Rakić¹ and
Jens C. Niemeyer^{1,2}

¹ Institut für Theoretische Physik und Astrophysik, Universität Würzburg,
Am Hubland, D-97074 Würzburg, Germany

² Institut für Astrophysik, Universität Göttingen, Friedrich-Hund-Platz 1,
D-37077 Göttingen, Germany

E-mail: dsimon@astro.uni-wuerzburg.de
jadamek@physik.uni-wuerzburg.de
rakic@astro.uni-wuerzburg.de
niemeyer@astro.physik.uni-goettingen.de

Abstract. In the context of bubble universes produced by a first-order phase transition with large nucleation rates compared to the inverse dynamical time scale of the parent bubble, we extend the usual analysis to non-vacuum backgrounds. In particular, we provide semi-analytic and numerical results for the modified nucleation rate in FLRW backgrounds, as well as a parameter study of bubble walls propagating into inhomogeneous (LTB) or FLRW spacetimes, both in the thin-wall approximation. We show that in our model, matter in the background often prevents bubbles from successful expansion and forces them to collapse. For cases where they do expand, we give arguments why the effects on the interior spacetime are small for a wide range of reasonable parameters and discuss the limitations of the employed approximations.

Keywords: Cosmological phase transitions, inflation, initial conditions and eternal universe, physics of the early universe

Contents

1	Introduction	2
2	Bubble nucleation in time-dependent settings	6
2.1	Lagrangian formulation	6
2.2	The complex time path formalism	7
2.3	Minkowski spacetime	8
2.4	de Sitter spacetime	9
2.5	More general FLRW spacetimes	9
2.6	Spacetimes with Big Bang singularity	10
3	Bubble propagation on dynamical backgrounds	12
3.1	Bubble wall and background spacetime	12
3.1.1	Interior: de Sitter	12
3.1.2	Bubble wall	13
3.1.3	Exterior: LTB and FLRW	13
3.2	Conditions for a valid junction	14
3.2.1	Equation of motion for the size and surface tension of the bubble	15
3.2.2	Evolution equations expressed in exterior coordinates	16
3.3	Bubble evolution on dynamical backgrounds	17
3.3.1	Exact solution in de Sitter/de Sitter spacetime	17
3.3.2	Numerical solution in de Sitter/LTB spacetime	17
3.3.3	Numerical solution in de Sitter/FLRW spacetime	22
4	Conclusions	25
	Appendix: Evolution equations in de Sitter/FLRW spacetime	27

1. Introduction

In the recent literature a lot of interest has been dedicated to the question of how inflationary models [1, 2] can be embedded into a general theory [3]. In this respect the emergence of the string theory landscape [4] has opened various possibilities and a completely new perspective. Due to flux compactification in string theory there can be a huge number of distinct vacua [5] in scalar field space without a unique physical selection mechanism available at present.

Classically, a field that is stuck in one vacuum would be trapped forever and could never move through the landscape. Quantum mechanically, the vacua are rendered metastable by the possibility for any field to tunnel to another (metastable) vacuum and thereby probe the landscape. The rate of tunneling naturally depends on the energy difference between the vacua and on the height and width of the potential barrier. The transition by pure tunneling can be described by the Coleman-De Luccia instanton [6]

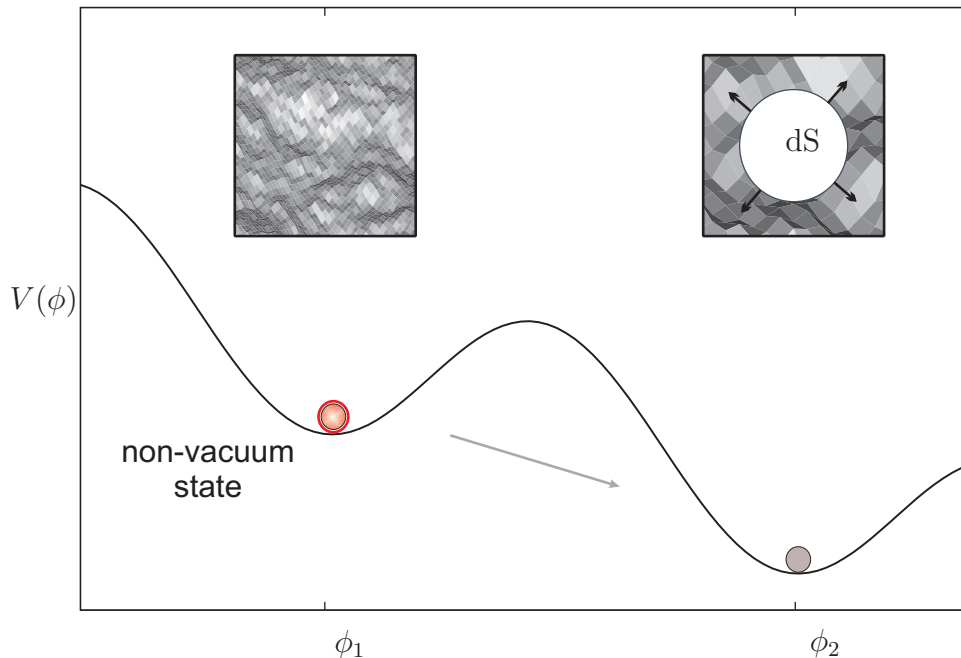


Figure 1. We investigate the effects on the tunneling and the evolution of bubbles of new vacuum when the precursor state is non-vacuum. The simplistic sketch shows such a tunneling event that can be imagined in the context of rapid tunneling in the landscape. We are interested in the case when tunneling is rapid enough such that the background had no time to relax to vacuum and is, for instance, undergoing a cosmological phase transition. This complication can be relevant in the context of chain inflation [10]–[18] or other models that invoke rapid tunneling, like e.g. DBI or resonance tunneling [19], [20]. For some particular examples of non-vacuum backgrounds (like e.g. radiation dominated FLRW or inhomogeneous LTB), we analyse the effects on the semiclassical tunneling rate as well as on the subsequent general relativistic evolution of the formed new vacuum bubbles.

whereas a transition over the barrier due to thermal fluctuations can be described by the Hawking-Moss instanton [7].

The Coleman-De Luccia process gives rise to the nucleation of spherically symmetric regions (bubbles) in space which are filled with new vacuum and expand into the old vacuum – a first-order phase transition. So, in the landscape multiple tunneling from multiple metastable vacua can occur, leading to different patches of spacetime undergoing coeval inflation in a variety of vacua. This process leads to a very complicated (fractal) large-scale structure of the universe that has been termed the attractor of eternal inflation. It is an attractor in the sense that statistical properties of the large-scale universe asymptotically do not depend on initial conditions [8].

The probability per unit four-volume for a tunneling to occur may be written as

$$\Gamma = A \exp(-2\text{Im}\mathcal{S}) , \quad (1)$$

where A is a determinantal factor and \mathcal{S} is the action of the instanton mediating the tunneling process. The prefactor A is notoriously hard to obtain and is usually assumed to be of order unity for most practical purposes. The instanton action \mathcal{S} can be obtained

by solving the field equations with appropriate boundary conditions. In many cases the layer separating the two phases can be thought of as a domain wall with a thickness that is small compared to the size of the bubble (‘thin-wall approximation’). With this assumption a calculation in Minkowski spacetime [9] yields $\text{Im}\mathcal{S} = 27\pi^2\sigma^4/4\epsilon^3$, with ϵ the latent heat and σ the energy density in the surface layer. It is often assumed that $\sigma \gg \epsilon$ (in Planck units) and thus tunneling is suppressed by a huge exponential factor, which implies extremely long lifetimes of the metastable vacua. However, any given point will eventually enter the decay chain, no matter what the odds are.

In this work we will study bubbles which nucleate from a non-vacuum initial state, that is inside pockets which do not obey the de Sitter symmetries because they are not vacuum dominated at the time when tunneling takes place, see Fig. 1. We look at tunneling from a precursor state that is, say, in a radiation or a matter dominated phase (but not yet vacuum dominated), and which produces an inflationary bubble of de Sitter vacuum. One may object that a large class [21, 22, 23, 24] of inflating spacetimes, if they include a positive cosmological constant, will always be vacuum dominated in the asymptotic future (the cosmic no-hair conjecture [7, 25, 26]). Together with the aforementioned long lifetimes of metastable vacua in the landscape this seems to render the question of bubble nucleation from anything other than the vacuum academic. However, there are recent proposals of inflation where tunneling between minima on the landscape occurs *rapidly*. This is the case, e.g., in the model of chain inflation‡ [10, 11, 12, 13, 14, 15, 16, 17, 18] or for non-standard tunneling on the landscape via DBI or resonance tunneling [19], [20]. In case of rapid tunneling – in chain inflation every transition only yields a fraction of an e-fold – the efficiency of the cosmic no-hair mechanism can be questioned. Therefore, we argue that the question of the consequences of rapid inflation through a pocket that has possibly not yet relaxed to pure vacuum deserves some attention. We will attack this problem in a twofold way. On the one hand, we will look at the tunneling itself and on the other hand, we will study the classical evolution of a vacuum bubble in a non-vacuum environment.

Concerning the former, one would for instance expect that the instanton action picks up some geometrical corrections due to the non-trivial background. Any such modifications are potentially interesting, since the tunneling rates are exponentially sensitive to them. We will show how one can assess the relevance of those effects, based on a comparison of characteristic time scales. Geometrical corrections become important if some dynamical time scale of the background is comparable to or smaller than the

‡ In chain inflation, tunneling occurs stepwise through a sequence of many minima. Chain inflation resurrects the old inflationary idea of a first-order phase transition but is able to solve the problem of graceful exit. Originally, this was accomplished because the fields were assumed to be coupled. The coupling is responsible for rapid tunneling: once a first tunneling has occurred the field increases the decay probability of its neighbor(s) further up in the landscape due to coupling. A chain reaction of rapid tunneling starts that eventually ends with a (slow) transition to true vacuum. However, chain inflation does not seem to allow for eternal inflation because it would not produce the right primordial density fluctuations [12]. In [13] a concrete realization of chain inflation on the string landscape that is driven by four form fluxes has been proposed.

characteristic time scale of the tunneling process, which is given by the bubble's proper nucleation radius. This may happen either when the nucleation radius is very large – but then tunneling rates are so small that the background geometry will relax to a de Sitter stage long before transition occurs – or when the background dynamics is characterized by some very short time scales.

The subsequent classical evolution of bubbles in such an environment will also be modified with respect to the vacuum case. We will study the propagation of vacuum bubbles in presence of i) homogeneously distributed matter, ii) matter with an inhomogeneous radial profile and iii) a fluid undergoing a second-order phase transition. These simple toy scenarios shall give a taste of the phenomenology which may result from non-vacuum initial states.

Besides for chain inflation, the results of this analysis can be important also for other scenarios. For instance, the influence of background inhomogeneity can be relevant in the context of landscape sampling by tunneling. While through resonant processes the tunneling rate on the landscape can be enhanced [20], inhomogeneous initial states may be of high importance for this sort of tunneling [27, 28]. The approach in our work is partly inspired by [29], where it was studied how an inhomogeneous and spherically symmetric background influences the classical evolution of an inflationary bubble of new vacuum immersed into it. In the limits of the used model it was claimed in [29] that ambient inhomogeneities do not alter the evolution of bubbles significantly as long as the weak energy condition is respected. On the other hand, this topic also touches the interesting issue of inhomogeneous initial conditions versus the onset of inflation, see e.g. [30, 31, 32, 33, 34, 35].

The paper is organized as follows. In section 2 we present results that show the influence of dynamical backgrounds on the nucleation rate of bubbles of new vacuum. To this end, we apply an extension of the usual semiclassical approach to cosmologically interesting time-dependent FLRW backgrounds such as power law inflation or radiation dominated universes. The nucleation rates are obtained in the thin-wall approximation by using a complex time path formalism. In section 3, we analyze the subsequent classical trajectory of bubbles. In addition to FLRW backgrounds§, we look at the evolution in an exact spherically symmetric and inhomogeneous spacetime containing also matter. The interior of the bubble is assumed to be de Sitter spacetime, as a first approximation to the inflationary phase of the patch of the universe that we are observing. The bubble evolution follows from the Israel junction method which is employed to join these spacetimes together. We ask whether signatures of the background can potentially be seen by an observer inside the bubble. In section 4 we summarize our results and give conclusions as well as some remarks on the limits of the used methods and an outlook. We use units $c = \hbar = G = 1$, and sign conventions for geometrical quantities in accordance with [36].

§ We thank Ben Freivogel for this suggestion.

2. Bubble nucleation in time-dependent settings

Quantum nucleation of bubbles is a very intricate problem, especially when effects of gravity have to be taken into account. Much of the literature on this topic focusses on the case of transitions between two vacua having different values of the cosmological constant. In this special case, a semiclassical calculation of the nucleation rate based on instanton methods has been presented by Coleman and De Luccia [6]. However, this calculation, as well as many alternative approaches developed by others (cf. e.g. [37]), heavily relies on a high degree of symmetry of spacetime, which is initially assumed to be in a pure vacuum state with the geometry of de Sitter spacetime. We therefore feel that the applicability of these results to cases where spacetime is not (or only approximately) in a vacuum state is in need of some clarification (see also the discussion in [38]).

A calculation of nucleation rates in arbitrary non-vacuum states, including all possible effects, is clearly beyond our capabilities. We will instead only take a small step away from the assumption of de Sitter symmetry and consider Friedmann universes in general, of which de Sitter spacetime is only a special case. We therefore retain many useful simplifications, in particular the assumption of homogeneity of space (but not of spacetime!), and the so-called ‘thin-wall approximation’. The cosmological expansion of the universe, however, follows a non-trivial dynamical law (the Friedmann equation), and we are interested in the effect of the *time-dependent* Hubble rate on the nucleation rate of bubbles, which will in turn itself become *time-dependent*.

To keep matters as simple as possible, we will consider the nucleation of a spherical bubble of new phase, and we will assume that its shell – the layer which separates the new phase from the old – is of negligible thickness compared to the size of the bubble. This amounts to the ‘thin-wall approximation’. The energy budget of the bubble consists of latent heat (the difference between the energy densities of the two phases) and surface tension. Throughout this section we will neglect gravitational backreaction of the bubble onto the spacetime geometry since we are primarily interested in the effects of cosmological expansion of the background, which is taken into account, and the treatment of the full gravitational problem would introduce too many additional complications.

2.1. Lagrangean formulation

Associated to the background spacetime is the Friedmann-Lemaître-Robertson-Walker (FLRW) line element

$$ds^2 = a^2(\eta) [-d\eta^2 + dr^2 + r^2 d\Omega^2] , \quad (2)$$

where we have assumed flat spatial sections. The conformal time η is related to cosmological (proper) time t by $dt = a d\eta$.

Spherical symmetry reduces the bubble dynamics to a 1 + 1 dimensional problem. Denoting the coordinate radius of the shell as \bar{r} , the shell trajectory $\bar{r}(\eta)$ follows from

the action

$$\mathcal{S} = \int d\eta \left[\frac{4\pi}{3} \epsilon a^4(\eta) \bar{r}^3(\eta) - 4\pi\sigma a^3(\eta) \bar{r}^2(\eta) \sqrt{1 - (\partial_\eta \bar{r}(\eta))^2} \right], \quad (3)$$

where ϵ and σ denote, respectively, the difference between the energy densities of the two phases (latent heat) and the surface energy density (surface tension) of the shell. As we have indicated above, this effective action does not take into account gravitational self-interaction of the bubble. In order to include some of these effects, one could add surface-surface, volume-volume, as well as surface-volume terms for gravitational energy.

The evolution of the scale factor a introduces an explicit time-dependence, giving rise to nucleation rates which will in general be time-dependent as well. A formalism for calculating semiclassical tunneling rates in time-dependent settings has been presented by Keski-Vakkuri and Kraus [39]. Its application to the present scenario will be worked out in detail in the following section.

2.2. The complex time path formalism

Our starting point is the classical equation of motion of the bubble, which can be found from eq. (3) as

$$4\pi\epsilon a^4 \bar{r}^2 - 8\pi\sigma a^3 \bar{r} \sqrt{1 - (\partial_\eta \bar{r})^2} = \frac{d}{d\eta} \left[4\pi\sigma \frac{a^3 \bar{r}^2 \partial_\eta \bar{r}}{\sqrt{1 - (\partial_\eta \bar{r})^2}} \right], \quad (4)$$

and we have dropped some labels in favor of simplified notation.

The classical trajectory after tunneling emanates from a classical turning point, where the canonical momentum

$$\bar{p} \equiv \frac{\partial \mathcal{L}}{\partial \partial_\eta \bar{r}} = 4\pi\sigma \frac{a^3 \bar{r}^2 \partial_\eta \bar{r}}{\sqrt{1 - (\partial_\eta \bar{r})^2}} \quad (5)$$

vanishes. It has been pointed out in [39] that by analytic continuation to complex η one can find a classical trajectory^{||} (in the complex η plane) that smoothly shrinks the bubble to zero size. To this end, it is useful to rewrite eq. (4) as an equation for $\eta(\bar{r})$:

$$4\pi\epsilon a^4 \bar{r}^2 \partial_{\bar{r}} \eta - 8\pi\sigma a^3 \bar{r} \sqrt{(\partial_{\bar{r}} \eta)^2 - 1} = \frac{d}{d\bar{r}} \left[4\pi\sigma \frac{a^3 \bar{r}^2}{\sqrt{(\partial_{\bar{r}} \eta)^2 - 1}} \right], \quad (6)$$

which, after some simplification, becomes

$$\frac{\epsilon}{\sigma} a \sqrt{(\partial_{\bar{r}} \eta)^2 - 1} = 2 \frac{\partial_{\bar{r}} \eta}{\bar{r}} + 3 \frac{\partial_\eta a}{a} - \frac{\partial_{\bar{r}}^2 \eta}{(\partial_{\bar{r}} \eta)^2 - 1}. \quad (7)$$

^{||} It turns out to be a special feature of time-dependent settings that this trajectory is not along a purely imaginary direction as would be the case in static settings, where, as a consequence, Euclideanization of time is a valid prescription.

We are looking for the solution with the boundary conditions

$$\bar{p}(\eta_0) = 4\pi\sigma \frac{a^3 \bar{r}^2}{\sqrt{(\partial_{\bar{r}}\eta)^2 - 1}} \Big|_{\eta=\eta_0} = 0, \quad \partial_{\bar{r}}\eta(0) = 0. \quad (8)$$

The first condition matches the solution to the turning point, from which on it remains on the real η axis for increasing \bar{r} . The second condition guarantees that the full spherically symmetric solution is regular at the origin $\bar{r} = 0$. Since η will depart from the real axis for radii smaller than the nucleation radius, it is clear that one also has to analytically continue the time-dependent scale factor a to the complex plane. These boundary conditions do not determine the solution entirely: we are still free to choose the ‘nucleation time’ η_0 . The ‘nucleation radius’, i.e. the coordinate radius of the bubble at the classical turning point, will accordingly be denoted as \bar{r}_0 , and fulfills $\eta(\bar{r}_0) = \eta_0$. This means that we have a one-parameter family of solutions labeled by their individual nucleation times. For each solution, the semiclassical tunneling rate is determined by the imaginary part of its action:

$$\Gamma(\eta_0) \sim \exp[-2\text{Im}\mathcal{S}(\eta_0)], \quad (9)$$

where it is again useful to write $\text{Im}\mathcal{S}(\eta_0)$ in terms of $\eta(\eta_0; \bar{r})$:

$$\text{Im}\mathcal{S}(\eta_0) = \text{Im} \int_0^{\bar{r}_0} d\bar{r} \left[\frac{4\pi}{3} \epsilon a^4(\eta(\eta_0; \bar{r})) \bar{r}^3 \partial_{\bar{r}}\eta(\eta_0; \bar{r}) - 4\pi\sigma a^3(\eta(\eta_0; \bar{r})) \bar{r}^2 \sqrt{(\partial_{\bar{r}}\eta(\eta_0; \bar{r}))^2 - 1} \right] \quad (10)$$

We have now all the tools to compute time-dependent tunneling rates. Let us now turn to some explicit examples.

2.3. Minkowski spacetime

Before dealing with time-dependent backgrounds, let us briefly review the situation in Minkowski spacetime. We can simply set $a = 1$ and $\eta = t$. Since we know that the solution has to be invariant under boosts, a natural ansatz for the trajectory is a hyperbola

$$\bar{r}^2 - (\eta - \eta_0)^2 = \bar{r}_0^2, \quad (11)$$

which yields

$$\eta(\eta_0; \bar{r}) = \eta_0 + \sqrt{\bar{r}^2 - \bar{r}_0^2}, \quad (12)$$

where the positive sign is chosen for the square root, corresponding to an expanding bubble for $\bar{r} > \bar{r}_0$. Inserting into eq. (7) one infers

$$\bar{r}_0 = \frac{3\sigma}{\epsilon}, \quad (13)$$

and one can check that this solution fulfills the boundary conditions (8). The imaginary part of its action can be found readily from eq. (10),

$$\text{Im}\mathcal{S}_{\text{Mink}} = \frac{\pi^2}{12} \epsilon \bar{r}_0^4 = \frac{27\pi^2 \sigma^4}{4\epsilon^3}, \quad (14)$$

which is exactly Coleman's result [9].

2.4. de Sitter spacetime

Our first example of an expanding universe will be de Sitter spacetime. Although it can actually be written in static coordinates, the FLRW metric with *flat* spatial sections has a scale factor which grows exponentially with time, $a = \exp(Ht)$. Written in conformal time this becomes $a = -1/H\eta$, where η runs from $-\infty$ to 0 as t runs from $-\infty$ to $+\infty$. In this case, eq. (7) reads

$$-\frac{\epsilon}{\sigma H \eta} \sqrt{(\partial_{\bar{r}} \eta)^2 - 1} = 2 \frac{\partial_{\bar{r}} \eta}{\bar{r}} - \frac{3}{\eta} - \frac{\partial_{\bar{r}}^2 \eta}{(\partial_{\bar{r}} \eta)^2 - 1}. \quad (15)$$

While finding the complete solution to this problem does not seem promising, it turns out that we can guess the relevant solution by sensibly generalizing eq. (12). Since de Sitter spacetime (in flat coordinates) has a constant expansion rate H , we expect that the *proper* nucleation radius should be independent of time. Now, if \bar{r}_0 is to be a *comoving* radius, it has to be divided by the scale factor, i.e. instead of eq. (13) we expect

$$\bar{r}_0 = a^{-1}(\eta_0) \frac{3\sigma}{\epsilon} = -H\eta_0 \frac{3\sigma}{\epsilon}. \quad (16)$$

Remarkably, choosing this nucleation radius is enough to have eq. (12) solve eq. (15) with the boundary conditions (8).

The integral of eq. (10) is still solvable, and its imaginary part is found to be

$$\begin{aligned} \text{Im} \mathcal{S}_{\text{ds}} &= \frac{\pi^2 \epsilon}{3H^4} \frac{\left(1 - \sqrt{1 + (3H\sigma/\epsilon)^2}\right)^2}{\sqrt{1 + (3H\sigma/\epsilon)^2}} \\ &= \frac{4\pi^2 \epsilon}{3H^4} \sinh^2 \frac{1}{4} \ln \left(1 + (3H\sigma/\epsilon)^2\right), \end{aligned} \quad (17)$$

which is independent of the choice η_0 for the time of nucleation. This means that the nucleation rate in de Sitter spacetime is time independent, which is a manifestation of the fact that de Sitter spacetime has no true dynamics. This expression reduces to the result of Minkowski spacetime eq. (14) in the limit of $H \rightarrow 0$. The first correction is of order H^2 and complies with the expansion obtained by Abbott, Harari and Park [40]. We can also take the limit $\epsilon \rightarrow 0$, which corresponds to the nucleation of a domain wall separating two degenerate vacua. One finds

$$\lim_{\epsilon \rightarrow 0} \text{Im} \mathcal{S}_{\text{ds}} = \frac{\pi^2 \sigma}{H^3}, \quad (18)$$

in complete agreement with a result obtained by Basu, Guth and Vilenkin [41].

2.5. More general FLRW spacetimes

Thus far we have only considered static spacetimes in order to get some experience using the new tools. Let us finally turn to more general spacetimes, where the expansion

rate is not assumed to be constant. A simple deformation of de Sitter expansion is given by power law inflation, where the scale factor grows as $a = (\eta_1/\eta)^{1+\alpha}$. For small deformation parameters α this is an exact slow-roll solution of inflation with a constant slow-roll parameter $-\partial_t H/H^2 \approx \alpha$. η_1 denotes an (arbitrary) point in time where the scale factor is normalized to unity. This spacetime is obviously not static, and we shall use this simple example to study effects of time-dependent cosmological expansion on tunneling rates. For power law inflation, eq. (7) reads

$$\frac{\epsilon}{\sigma} \left(\frac{\eta_1}{\eta} \right)^{1+\alpha} \sqrt{(\partial_{\bar{r}}\eta)^2 - 1} = 2 \frac{\partial_{\bar{r}}\eta}{\bar{r}} - 3 \frac{1+\alpha}{\eta} - \frac{\partial_{\bar{r}}^2\eta}{(\partial_{\bar{r}}\eta)^2 - 1} . \quad (19)$$

We have been unable to find an analytic solution to this equation and therefore decided to treat it numerically. Using the boundary conditions (8) one can find numerical solutions for any choices of α , η_0/η_1 and ϵ/σ . A parameter study of the tunneling rates reveals the following picture. There are now three different time scales in the problem. The inverse expansion rate $H^{-1}(\eta)$ gives the time scale on which the background (scale factor) changes significantly. But there is now another time scale related to the change of the expansion rate itself (higher order derivatives of the expansion rate are zero in power law inflation). These two time scales have to be compared to the ‘bubble crossing time’, which we define by the nucleation radius divided by the speed of light, or roughly $3\sigma/\epsilon$ in our units.

If the bubble crossing time is the smallest time scale of the problem, the tunneling rate is well approximated by the result of Minkowski spacetime, eq. (14). However, if the bubble crossing time is not much smaller than the Hubble time at nucleation, $H^{-1}(\eta_0)$, there are two different possibilities. Either the characteristic time scale for the *change* of the expansion rate, $|\partial_t H/H|^{-1}$, is still much larger than the bubble crossing time – then we are in a regime where a quasistatic approximation is valid such that a good estimate for the tunneling rate can be obtained from eq. (17) by setting $H = H(\eta_0)$. Or the bubble crossing time cannot be regarded as small with respect to any other time scale. In this case, the tunneling process ‘feels’ the changing expansion rate, and the decay rate is modified significantly. Our numerical study clearly indicates that the tunneling rate is enhanced compared to the quasistatic estimate. We believe that this is related to the fact that the expansion rate decreases with time. Instead of setting $H = H(\eta_0)$ in eq. (17), one should *average* the expansion rate over an interval of one bubble crossing time prior to nucleation. Using this averaged expansion rate in eq. (17) turns out to give a much better estimate for the actual tunneling rate, cf. Fig. 2.

2.6. Spacetimes with Big Bang singularity

An interesting case which is also relevant for the chain inflation scenario is a universe filled with radiation and some vacuum energy, such that radiation dominates its early evolution, while it approaches a vacuum de Sitter phase at later time. If we neglect the brief era of matter domination, this is also a good model for our present universe (after reheating has taken place). During the radiation era, the Hubble rate drops rapidly,

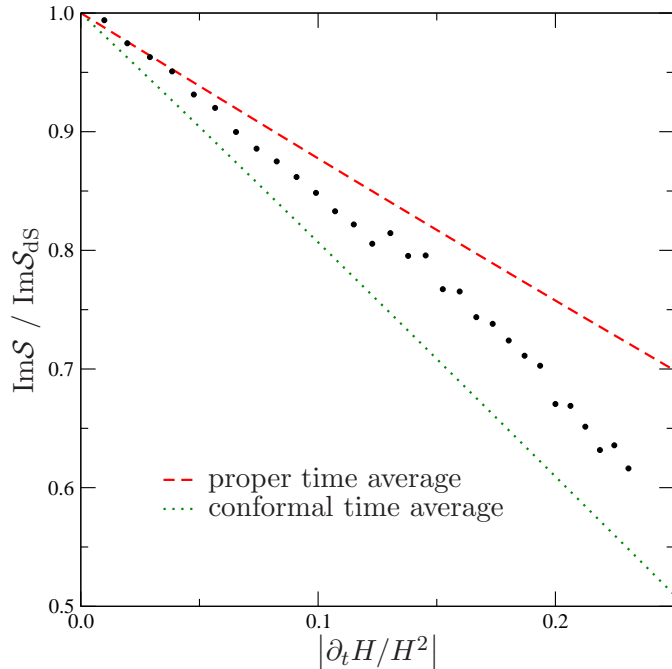


Figure 2. Numerical values for the imaginary part of the action \mathcal{S} for tunneling solutions with proper nucleation radius $3\sigma/\epsilon = 2H^{-1}(\eta_0)$, as a function of the slow roll parameter $\partial_t H/H^2$. The values are normalized to the ‘quasistatic approximation’, which is obtained from eq. (17) by setting $H = H(\eta_0)$. Thus, in this approximation only instantaneous dynamical parameters are taken into account. The tunneling process, however, has a characteristic time scale given by the light-travel time across the bubble. Hence it is more appropriate to take into account some *average* dynamics of the background. In a crude way, this can be accomplished by using an averaged expansion rate to evaluate the tunneling probability in the quasistatic approximation. The dashed red line is obtained from a *proper time average* of H taken over an interval $\Delta t = 3\sigma/\epsilon$ before nucleation, whereas the dotted green line is obtained from a *conformal time average* taken over an interval $\Delta\eta = \Delta t/a(\eta_0)$.

and assuming the vacuum is metastable, one might wonder if this affects tunneling rates as described above. We can answer this question by comparing the relevant time scales. If the universe is sufficiently flat, $a \propto t^{1/2}$ as long as radiation dominates over vacuum energy. Note that the universe has a Big Bang singularity at $t = 0$ as long as reheating and any kind of cosmology before the radiation era is not taken into account. Hence, there exists a particle horizon of size $\sim t$. Also both the Hubble time and the characteristic time scale for the change of the Hubble rate are of order $\sim t$. Since even tunneling cannot violate causality, bubbles larger than the particle horizon cannot be produced, at least not in the semiclassical picture we are using here. This means that the bubble crossing time can never be much larger than the other relevant time scales, and thus we expect corrections to the tunneling rates to be small in general. Moreover, a numerical study indicates that the tunneling rates for bubbles whose nucleation radius is comparable to the size of the particle horizon become sensitive to the dynamics of the scale factor up to the vicinity of the Big Bang, such that details of reheating and even earlier cosmology become relevant.

As soon as vacuum energy begins to dominate, the time scale on which the expansion rate changes tends to infinity quite rapidly as the Hubble rate approaches a constant. Hence, for the late part of the evolution, we expect the de Sitter approximation to be good. Note, however, that a particle horizon still exists and that bubbles should not exceed the horizon size at any time as long as causal physics is at play. To eliminate

this ‘horizon problem’[¶], one has to change the details of the model near the Big Bang singularity to include any cosmology preceding the era of radiation domination.

3. Bubble propagation on dynamical backgrounds

In this section we will explore the effect of background irregularities on the evolution of the bubble and whether these effects can potentially be seen by an observer inside the bubble. To this end we will follow a somewhat different route than in the preceding section, where we ignored gravitational backreaction of the bubble. In order to include this backreaction, we will follow the approach used in [29] and assume that the bubble wall separates spacetime into two parts, described by different metrics and containing different matter. These two parts, for convenience called interior and exterior part, are approximated by the manifolds \mathcal{M}_- and \mathcal{M}_+ and are joined along a common timelike, spherically symmetric hypersurface Σ which represents the bubble wall. Since the work of Israel [42] there exists a well established formalism for joining manifolds along a common boundary, known as the Israel junction conditions. Once \mathcal{M}_- and \mathcal{M}_+ are given, the evolution of the bubble wall uniquely follows from these conditions. Moreover, by this construction, the resulting spacetime is a solution to Einstein’s field equations.

For the interior part we use de Sitter spacetime (which can be thought of as an approximation to the inflationary phase of our observable patch of the universe) and for the exterior part two different cases will be considered. We will study the evolution of vacuum bubbles in an inhomogeneous background for which the exterior part is approximated by the spherically symmetric Lemaître-Tolman-Bondi (LTB) spacetime [43, 44, 45]. To maintain spherical symmetry it is assumed that the bubble nucleates in the center of the LTB model. In a similar vein, we will also explore the evolution of vacuum bubbles when the exterior part is given by a FLRW universe filled with a fluid which at some time undergoes a smooth (second-order) phase transition, e.g. from $w = -1$ to $w = 1/3$, or vice versa.

In the first subsection we will introduce the description of the bubble wall and the interior and exterior parts of spacetime. Thereafter we will give a concise guide on how to calculate the junction equations and write them down explicitly for the cases of our interest. Finally we will solve these equations numerically and discuss the results.

3.1. Bubble wall and background spacetime

3.1.1. Interior: de Sitter The interior of the bubble is assumed to be in a de Sitter phase with vacuum energy density given by $\Lambda/(8\pi)$. We employ the flat slicing in which the metric is given by

$$ds^2 = -dt^2 + \exp\left(2\sqrt{\Lambda/3} t\right) (dr^2 + r^2 d\Omega^2) , \quad (20)$$

[¶] Actually, this is nothing but the good old horizon problem of standard Big Bang cosmology in a new guise, and therefore it can be solved in the same spirit.

and stress-energy is given by $T_{\mu\nu} = -\Lambda g_{\mu\nu}$. All quantities should carry the index $(-)$ which indicates that they belong to \mathcal{M}_- . For convenience we write these indices only when necessary, hoping that it will be clear from the context which quantities are meant.

3.1.2. Bubble wall The timelike, spherically symmetric hypersurface separating the interior and exterior parts of spacetime, the bubble wall, is described by the metric

$$ds^2 = -d\tau^2 + R^2 d\Omega^2 . \quad (21)$$

Though it has been shown [46] that the stress-energy of a wall which separates regions of different vacua will solely be given by the surface tension, it is not clear whether this conclusion is valid when matter is present. However, in lack of a field theoretic description, we assume that stress-energy is given by

$$S_{ij} = -\sigma h_{ij} . \quad (22)$$

where h_{ij} is the metric tensor of (21). The equations of motion of the proper radius R and surface tension σ of the bubble will be given by the junction conditions.

3.1.3. Exterior: LTB and FLRW

LTB spacetime In order to explore the evolution of a bubble in an inhomogeneous background we use an LTB ansatz. In comoving coordinates a suitable metric [47] can be given in the form

$$ds^2 = -dt^2 + \frac{(r\partial_r a(t,r) + a(t,r))^2}{1 + 2E(r)} dr^2 + a^2(t,r)r^2 d\Omega^2 , \quad (23)$$

with $2E(r) > -1$ but otherwise arbitrary. From Einstein's equations with a dust source $T_{\mu\nu} = \rho\delta_\mu^t\delta_\nu^t - \Lambda g_{\mu\nu}$, we obtain the equation of motion of the scale factor

$$\left(\frac{\partial_t a}{a}\right)^2 - \frac{2E}{a^2 r^2} = \frac{2M}{a^3 r^3} + \frac{\Lambda}{3} . \quad (24)$$

Here, $M(r)$ is the first integral of motion which corresponds to the active gravitational mass within a sphere of coordinate radius r . Once the scale factor is known, the dust density ρ is determined by

$$8\pi\rho = \frac{2\partial_r M}{a^2 r^2 (r\partial_r a + a)} . \quad (25)$$

FLRW spacetime In addition, we want to study the motion of bubbles in a background which undergoes a phase transition. Therefore a flat FLRW spacetime is employed, a comoving coordinate system of which is

$$ds^2 = -dt^2 + a^2(t) (dr^2 + r^2 d\Omega^2) , \quad (26)$$

with stress-energy given by

$$T_{\mu\nu} = (\rho + p)\delta_\mu^t\delta_\nu^t + pg_{\mu\nu} - \Lambda g_{\mu\nu} . \quad (27)$$

The evolution of this background follows from the Friedmann equation

$$\left(\frac{\partial_t a}{a}\right)^2 = \frac{8\pi}{3}\rho + \frac{\Lambda}{3}, \quad (28)$$

and continuity equation

$$\partial_t \rho + 3\frac{\partial_t a}{a}(\rho + p) = 0. \quad (29)$$

To look at the influence of a phase transition in the background on the evolution of the bubble, we artificially⁺ introduce an abrupt change in the equation of state $p = w\rho$ via

$$w(t) = -\frac{1}{3}(1 \pm 2 \tanh(\gamma_{\text{pt}}(t - t_{\text{pt}}))) . \quad (30)$$

to model a nearly instantaneous (on time scale $\gamma_{\text{pt}}^{-1} \ll H^{-1}$) phase transition at $t = t_{\text{pt}}$ from $w = -1$ to $w = 1/3$ ('reheating') and vice versa. Solutions to equations (28) and (29) can not be given in closed form and will be obtained numerically.

3.2. Conditions for a valid junction

The problem of joining manifolds across a common boundary has been lucidly explained in the work of Israel [42]. For a nice introduction see also the textbooks [48, 49]. Two conditions arise in the course of joining two manifolds. The first junction condition requires the induced metrics $h_{ij} = g_{\mu\nu}e_i^\mu e_j^\nu$ to coincide on Σ

$$[h_{ij}] \equiv h_{ij}^+|_\Sigma - h_{ij}^-|_\Sigma = 0. \quad (31)$$

The second junction states that, whenever there is a discontinuity in the extrinsic curvature of Σ as seen from \mathcal{M}_\pm , a surface layer of stress-energy S_{ij} , given by

$$8\pi S_{ij} = [K_{ij}] - h_{ij}[K] \quad (32)$$

will be present. Therefore the proposed stress-energy on the bubble wall (22) has to be identified with the difference in the extrinsic curvature. The components of the extrinsic curvature tensor K_{ij} are defined as the covariant derivative of the vector e_j^μ along e_i^ν projected onto the surface normal

$$K_{ij} = n_\alpha \Gamma_{\mu\nu}^\alpha e_i^\mu e_j^\nu. \quad (33)$$

Once the projectors $e_i^\mu = \partial x^\mu / \partial y^i$ are known, the normal vector of Σ can be obtained by the conditions

$$n_\mu n^\mu = 1 \quad \text{and} \quad n_\mu e_i^\mu = 0 \quad (34)$$

up to a sign which determines how \mathcal{M}_- and \mathcal{M}_+ are stuck together. We choose this sign such that

$$n_\mu = \sqrt{g_{rr}}(-\dot{r}, \dot{t}, 0, 0), \quad (35)$$

⁺ A universe with two or more components with different equations of state, like e.g. radiation and cosmological constant, actually has one or several intrinsic phase transitions. However, these transitions are very gentle and would probably only produce a minuscule effect.

where a dot refers to a partial derivative with respect to τ . This choice implies that in \mathcal{M}_- , radii increase towards Σ and in \mathcal{M}_+ , radii decrease towards Σ . The continuity equation

$$\nabla_i S_j^i + \left[T_\beta^\alpha n_\alpha e_j^\beta \right] = 0 . \quad (36)$$

is not independent of the two equations resulting from (32) and will be used to substitute one of these. We consider exterior stress-energy given by a perfect fluid and interior by a cosmological constant. Therefore the τ component provides the following first order equation for σ

$$\dot{\sigma} = (\rho + p) \sqrt{g_{rr}} \dot{r} . \quad (37)$$

In the next subsections we will write down these equations for LTB spacetime.

3.2.1. Equation of motion for the size and surface tension of the bubble By virtue of spherical symmetry of the bubble wall, angular coordinates can be identified and the time and radial coordinate can be parameterized by the proper time of the bubble $(t(\tau), r(\tau))$. We write down the equations for the LTB part and relegate the FLRW equations to the appendix. The conditions of the first junction turn out to be

$$ar = R, \quad \dot{t}^2 = 1 + \frac{(r\partial_r a + a)^2}{1 + 2E} \dot{r}^2 . \quad (38)$$

We will make use of the $\theta\theta$ -component of the second junction condition which yields

$$4\pi\sigma R = \sqrt{\dot{R}^2 + 1 - \frac{\Lambda_-}{3}R^2} - \sqrt{\dot{R}^2 + 1 - \frac{2M}{R} - \frac{\Lambda_+}{3}R^2} . \quad (39)$$

Solving for the derivative we obtain the more convenient form

$$\frac{1}{2}\dot{R}^2 + V = -\frac{1}{2} , \quad (40)$$

with $2V$ given by

$$2V = - \left[\frac{\Lambda_-}{3} + \left(\frac{\Lambda_+ - \Lambda_-}{24\pi\sigma} + 2\pi\sigma \right)^2 \right] R^2 - \left(1 + \frac{\Lambda_+ - \Lambda_-}{48\pi^2\sigma^2} \right) \frac{M}{R} - \frac{M^2}{16\pi^2\sigma^2 R^4} . \quad (41)$$

If $M = \text{const}$ all coefficients in the potential are constant and we recover the Schwarzschild-de Sitter model which has been discussed in [46, 50, 51, 52].

However, since we want to introduce an exterior matter density, M will no longer be constant, i.e. $M(r) = M(R/a)$ and the scale factor of the ambient spacetime will enter the equation. In this way the motion of the surface becomes sensitive to the presence of matter in the background.

Note that (23) is covariant under a rescaling of the radial coordinate. Together with $\partial_r M > 0$ this allows one to define a radial coordinate such that $M(r) = \frac{4\pi}{3} A r^3$ where A is a constant. The potential becomes

$$2V = - \left[\frac{\Lambda_-}{3} + \left(\frac{A}{3a^3\sigma} + \frac{\Lambda_+ - \Lambda_-}{24\pi\sigma} + 2\pi\sigma \right)^2 \right] R^2 . \quad (42)$$

and the equation of motion for the surface tension is

$$\dot{\sigma} = \rho \frac{r\partial_r a + a}{\sqrt{1+2E}} \dot{r} \dot{t}. \quad (43)$$

It is restricted by equation (39) to

$$4\pi\sigma < \sqrt{\frac{8\pi A}{3a^3} + \frac{\Lambda_+ - \Lambda_-}{3}} \equiv \sqrt{\frac{8\pi}{3}}\epsilon. \quad (44)$$

Here ϵ is the difference in energy density between inside and outside. This bound is a direct consequence of the geometry that was fixed by the sign of the normal vector (35).

3.2.2. Evolution equations expressed in exterior coordinates Since the background dynamics of the LTB (and FLRW) part of the spacetime can be obtained only numerically all equations will be solved in these coordinates in the first place. Making use of the junction conditions we are able to write down the evolution equations in terms of the exterior coordinates. After a solution to these equations has been obtained, the matching conditions will be employed again to express the evolution in terms of the interior coordinates. Like before, we explicitly write down the expressions for the LTB part and provide the FLRW equations in the appendix.

Let $\bar{r}(t)$ be the bubble radius in these coordinates. Writing $\dot{R} = \dot{t} \frac{d}{dt}(a\bar{r})$ we can solve for $\partial_t \bar{r}$ and obtain

$$\partial_t \bar{r} = \frac{-(1+2E)\bar{r}\partial_t a + \sqrt{(1+2E)(1+2V)((\bar{r}\partial_t a)^2 - 2E + 2V)}}{(\bar{r}\partial_r a + a)(2E - 2V)}. \quad (45)$$

where we have chosen a positive sign of the square root because we are interested in solutions of physically growing bubbles, i.e. $\dot{R} \geq 0$. The equation for σ (37) can as well be converted to LTB coordinates

$$\partial_t \sigma = \rho \frac{(\bar{r}\partial_r a + a) \partial_t \bar{r}}{\sqrt{1+2E - (\bar{r}\partial_r a + a)^2 (\partial_t \bar{r})^2}}. \quad (46)$$

The surface tension becomes time dependent. It increases when the comoving radius of the bubble increases, i.e. it collects matter from the background, and if the bubble shrinks it will exactly provide the amount of matter density determined by the background. This is a limitation of the spacetime junction approach, which in the present form does not capture the physics of matter transfer across the junction surface. Physically we would expect that dust would actually penetrate into the bubble, as one can convince oneself by looking at the geodesics of ‘test particles’. However, interior and exterior parts of spacetime are fixed ab initio and cannot be changed by the motion of the bubble. Bearing with this limitation, we continue our analysis and will give an outlook on this issue in our conclusions.

For now, equations (45) and (46) completely determine the evolution of the bubble in exterior coordinates.

3.3. Bubble evolution on dynamical backgrounds

In this section we explore the propagation of bubbles on dynamical backgrounds. We start with an exact solution of a de Sitter/de Sitter spacetime and continue with the numerical solutions obtained for the de Sitter/LTB and de Sitter/FLRW spacetimes.

3.3.1. Exact solution in de Sitter/de Sitter spacetime We solve equations (45) and (46) for the case that both spacetimes are de Sitter with cosmological constants given by Λ_{\pm} . Then $M = 0$ and we employ the flat slicing where also $E = 0$. Since there is no matter in the background it follows from equation (46) that $\sigma = \text{const}$. The potential V reduces to

$$2V = - \left[\frac{\Lambda_{\pm}}{3} + \left(\frac{\epsilon}{3\sigma} + 2\pi\sigma \right)^2 \right] R^2 . \quad (47)$$

For further convenience we define

$$u_{\pm}^2 \equiv \frac{3}{\Lambda_{\pm}} \left(\frac{\epsilon}{3\sigma} \mp 2\pi\sigma \right)^2 , \quad (48)$$

such that $2V = -H_{\pm}^2(1 + u_{\pm}^2)R^2$, where $H_{\pm}^2 = \Lambda_{\pm}/3$. The solution is valid in \mathcal{M}_{-} and \mathcal{M}_{+} , with the corresponding quantities (u_{-}, Λ_{-}) and (u_{+}, Λ_{+}) respectively. Equation (45) becomes

$$\frac{2V(a\bar{r})}{H} \frac{\partial_t \bar{r}}{\bar{r}} = 1 - |u| \sqrt{-2V(a\bar{r}) - 1} . \quad (49)$$

which, when rewritten as a differential equation for V , can be solved by separation of variables. Solving for \bar{r} yields

$$\bar{r}(t) = \sqrt{u^{-2} + (\exp(-Ht) - 1)^2} H^{-1} . \quad (50)$$

For convenience we normalized the scale factor at the time $t = t_0$ when $\partial_t \bar{r}(t_0) = 0$ and took $t_0 = 0$ without loss of generality. This implies

$$\bar{r}_0^{\pm} = \left| \frac{\epsilon}{3\sigma} \mp 2\pi\sigma \right|^{-1} . \quad (51)$$

After $t = t_0$ the bubble accelerates and converges to $\bar{r}(t \rightarrow \infty) = \sqrt{1 + u^2} \bar{r}_0$, see Fig. (3). We conclude with the remark that (50) reduces to the solution found in (16) in the limit of $G \rightarrow 0$.

3.3.2. Numerical solution in de Sitter/LTB spacetime The goal of this section is to understand the influence of ambient inhomogeneities on the motion of the bubble wall. The first step into the numerics of the bubble is solving the dynamics of the background.

For an intuitive approach we define $2E(r) = -k(r)r^2$ where the profile k may be interpreted as the local spatial curvature. Then, the coordinate size of the spatial section, if finite, is determined by $k(r_{\max})r_{\max}^2 = 1$. In addition, we have to specify the initial value of the scale factor $a_0(r) \equiv a(t_0, r)$ which will in general depend on the radial coordinate. Instead, one may equivalently choose the initial dust density $\rho_0(r) \equiv \rho(t_0, r)$, which defines $a_0(r)$ via equation (25). Thus, in coordinates where $M(r) = \frac{4\pi}{3}Ar^3$, spatial

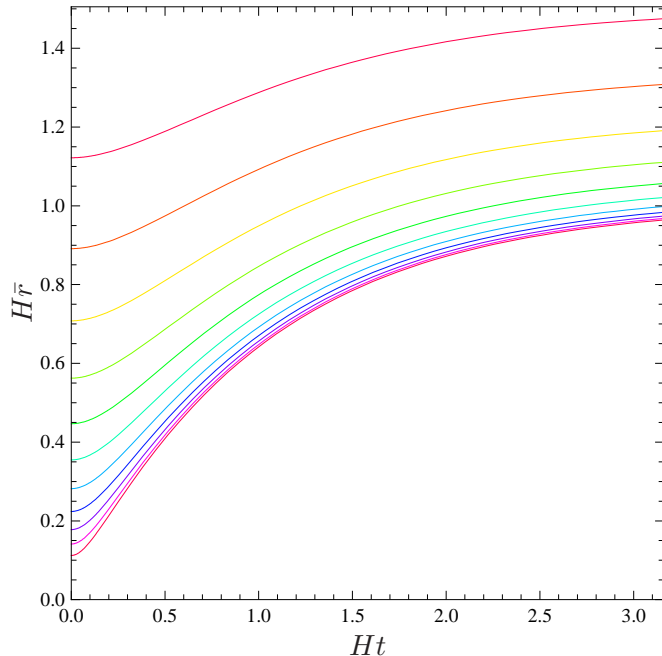


Figure 3. Trajectories of the bubble wall in the flat slicing of de Sitter/de Sitter spacetime for different values of u ; the parameter u (48) encodes the dependency on Λ_{\pm} and the surface tension σ . The bubble expands accelerated from coordinate radius $\bar{r}_0 = u^{-1}H^{-1}$ but converges to the finite coordinate radius $\sqrt{1 + u^2}\bar{r}_0$ in the limit $t \rightarrow \infty$. The trajectory is shown in de Sitter coordinates rather than in physical quantities (proper radius R vs. proper time τ) to make comparison to our later results easier.

inhomogeneity of the LTB spacetime is incorporated in the functions k and ρ_0 . In the limit where k and ρ_0 are constant the model becomes homogeneous.

After both functions have been specified, the partial differential equation (24) can directly be integrated at each r . When a solution is found its validity has to be checked. If not $\partial_r(ar) > 0$, the weak energy condition $\rho \geq 0$ is violated by the occurrence of a shell-crossing singularity. This actually restricts the curvature profile k , since, if too steep, it disturbs the background massively such that the dust density will violate the weak energy condition at some time. We evolve the system until the background space has expanded for about 4 e-folds.

The initial time of the analysis is $t = t_0$ where $\partial_t \bar{r}(t_0) = 0$. t_0 will be referred to as the time of nucleation of the bubble. The nucleation radius is determined by the parameters $A, \Lambda_+, \Lambda_-, \sigma_0$. It can be inferred from equation (45) which we rearrange to

$$\frac{1}{\bar{r}_0^2} = k(\bar{r}_0) + a_0^2(\bar{r}_0) \left(\frac{\epsilon_0}{3\sigma_0} - 2\pi\sigma_0 \right)^2. \quad (52)$$

Note that the initial difference in energy density ϵ_0 includes the initial dust density ρ_0 , which can be a function of \bar{r}_0 , too. This equation illustrates the route that we will follow. There are two possibilities, via the functions k and ρ_0 , to introduce inhomogeneity in the LTB model. These two cases are considered independently, meaning that one of the two terms on the right hand side will be independent of r . In case there is more than one solution to the equation the smallest positive value will be taken.

Note also that the proper kinetic energy of the bubble at nucleation is proportional to $\dot{R}^2|_{t=t_0} = H_0^2 R_0^2$, where $H_0 \equiv \frac{\partial_t a}{a}(t_0, \bar{r}_0)$ and $R_0 = a_0(\bar{r}_0)\bar{r}_0$.

Homogeneous limit The first thing we will explore is not the effect of inhomogeneity, but simply what happens when the bubble nucleates in a background where, in addition

to vacuum energy density, some dust is present. To keep things simple we refrain from adding any curvature at this stage and set $k = 0$ and $a_0(r) = 1$. The spatial sections of LTB spacetime become homogeneous and reduce to the FLRW limit. Henceforth, we will always assume that at nucleation dust density shall exceed exterior vacuum energy, and for definiteness we choose $8\pi A/3 = 10^{-4}$ and $\Lambda_+/3 = 10^{-5}$ in accordance with [29].

It is important to note that this setup already has a significant effect on the evolution of the bubble. Whereas a bubble that nucleates in vacuum always begins to expand, this is no longer guaranteed as soon as considerable amounts of matter are present in the environment. This can be seen by the following argument. The force which accelerates the shell has two contributions: one from the surface tension, which is always directed inwards, and one from the pressure difference between the interior and exterior fluid. In the case where both fluids are mere cosmological constants it is easy to show that the pressure force can sustain the surface tension and will push the shell outwards. However, if the exterior fluid is mainly composed of pressureless dust, at some point surface tension will outrun pressure support and the bubble will be forced to collapse.

To make this statement more quantitative we can take another derivative of eq. (45) and examine the behavior of the bubble when $\partial_t \bar{r} = 0$. In the homogeneous limit one finds

$$\partial_t^2 \bar{r} \Big|_{\partial_t \bar{r}=0} = \frac{1}{a} \left(\frac{\Lambda_+ - \Lambda_-}{24\pi\sigma} - 2\pi\sigma - \frac{2\rho}{3\sigma} \right). \quad (53)$$

The sign of $\partial_t^2 \bar{r}$ depends on how σ^2 and ρ compare to the latent heat of the vacuum, $\epsilon_{\text{vac}} \equiv (\Lambda_+ - \Lambda_-)/8\pi$. The bubble can only expand into the ambient spacetime if ρ is not too large. In particular, one can never have an expanding bubble during a matter dominated phase*. This strongly limits the possibility to study the propagation of bubbles into inhomogeneous matter with the current approach, since the exterior spacetime has to be vacuum dominated in order to allow the bubble to propagate towards the inhomogeneity in the first place. We have summarized the behavior of freshly nucleated bubbles of vacuum within a dust environment in Fig. 4.

We numerically calculated the trajectories of bubbles in a dust dominated background. As expected by the argument above, in contrast to the de Sitter case, bubbles contract as seen from the exterior perspective (Fig. 5, left). In fact some bubbles contract so fast that the growth of their physical size is decelerated, i.e. their proper kinetic energy decreases. Our results show that it will even decrease to zero for small bubbles with $H_0 \bar{r}_0 \lesssim 1$. In this case the proper kinetic energy becomes imaginary and the evolution of the bubble had to be stopped. When $\bar{r}_0 \gtrsim H_0^{-1}$ they retain some proper kinetic energy but nevertheless shrink in exterior coordinates and converge to a coordinate radius which is smaller than the coordinate radius of nucleation. For bubbles

* Note that this was not at all an issue in section 2, since background spacetime was assumed spatially homogeneous and any dust would therefore permeate the bubble. In the present setup, however, the interior is assumed to be completely empty except for a possible cosmological constant. In this sense, the issue is one of initial conditions.

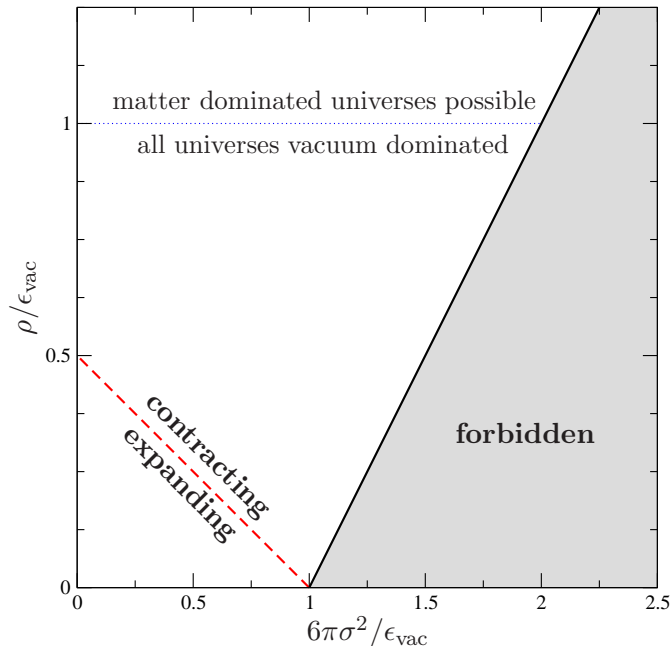


Figure 4. This plot characterizes the early-time behavior of a vacuum bubble after it was nucleated at rest in the comoving frame of an exterior flat FLRW spacetime with dust and cosmological constant. With respect to an exterior comoving observer, the bubble shows different behavior in different regions of the σ^2 - ρ -plane, which is drawn in units of $\epsilon_{\text{vac}} \equiv (\Lambda_+ - \Lambda_-)/8\pi$. The shaded region is forbidden for our choice of junction because σ there violates the bound (44). If the energy density of dust ρ is chosen above the dashed red line, the bubble starts to contract. This includes all matter dominated universes $\rho > \rho_{\text{vac}} \equiv \Lambda_+/8\pi$ since we assume $\Lambda_+ > \Lambda_- \geq 0$, which implies $\rho_{\text{vac}} \geq \epsilon_{\text{vac}}$. Below the dashed red line the bubble starts to expand into the ambient spacetime. This includes all vacuum de Sitter spacetimes since they are found on the line $\rho = 0$. Below the dotted blue line, all universes are vacuum dominated.

larger than $2H_0^{-1}$, even if they fulfill the bound (44) initially, the dust density in the background drops faster than the surface tension of the bubble such that the bound will be violated soon.

Note also that after $\sqrt{\Lambda_+/3} t_{\text{eq}} \simeq 0.4$ the bubble moves on a vacuum dominated background. The contour plot in 5 illustrates the fate of a bubble in dependence of the parameters (Λ_0, σ_0) .

Inhomogeneous dust density We now explore possible effects of inhomogeneity by the introduction of an initial dust distribution $\rho_0(r)$. The bubble may nucleate either in an overdense or in an underdense region of space. It is not very revealing to consider a radially decreasing dust profile, because the dust will be rarefied by the expansion of the background anyway. Therefore we will have a look at radially increasing dust profiles only. For a given $\rho_0(r)$, the initial scale factor is determined by

$$a_0^3(r) = \frac{3A}{r^3} \int \frac{r^2}{\rho_0(r)} dr. \quad (54)$$

We will consider the profile

$$\rho_0(r) = Ar^3/r_A^3 \quad (55)$$

with $r_A = (\Lambda_+/3)^{-1/2}$. We expect that small bubbles with $\bar{r}_0 \ll r_A$ will begin to expand initially because they will find themselves in a vacuum dominated background, whereas large bubbles with $\bar{r}_0 \gtrsim r_A$ are in a matter dominated background with their subsequent

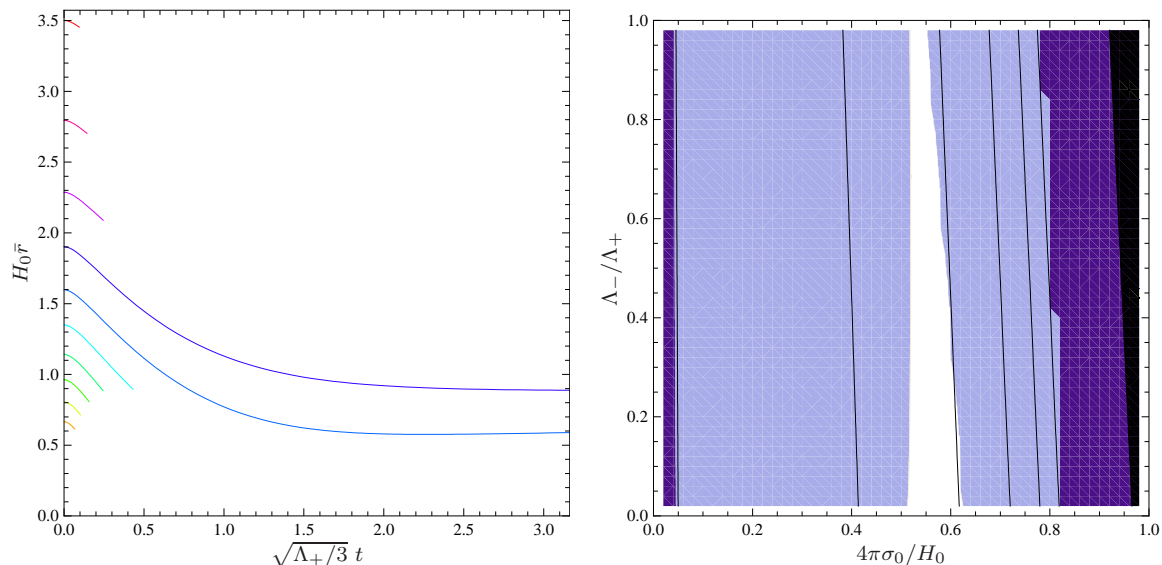


Figure 5. Results obtained for the homogeneous limit of the LTB model with $k = 0$ and $a_0(r) = 1$. Left figure: Trajectories of the bubble wall for several values of the surface tension $0.3H_0 \leq 4\pi\sigma_0 \leq 0.75H_0$ and $\Lambda_- = 0.1\Lambda_+$. The fate of the bubble depends on the nucleation size. Small bubbles contract in LTB coordinates until their proper kinetic energy becomes zero, i.e. $\dot{R} = 0$ and the equation of motion becomes imaginary. The greater the bubble the more likely it sustains kinetic energy until the background is dominated by Λ_+ and it converges to some finite coordinate radius. Right figure: Fate of a bubble in dependence of the parameters σ_0, Λ_- . We looked in the region of parameter space where the nucleation radius of the bubble is within $0.1 < H_0 \bar{r}_0 < 5$. The black lines are lines of constant kinetic energy and nucleation radius $H_0 \bar{r}_0 = (0.1, 1, 2, 3, 4, 5)$. The black shaded region is considered to be unphysical since equation (44) is not fulfilled there already initially. In the region shaded light blue, bubbles either contract until $\dot{R} = 0$, or they hit the geometrical bound (44). Neither occurs in the white region in which bubbles ‘survive’ and come to rest at a finite coordinate radius.

evolution being much like in the homogeneous limit discussed before. Although the initial dust profile is increasing, expanding bubbles propagate into regions of lower density due to the expansion of the background, see Fig. 6.

Inhomogeneous curvature The other possibility is to incorporate inhomogeneity in the neighborhood of the bubble via a curvature profile k . However, in view of the results obtained in the homogeneous limit, we state that the bubble will hardly be able to propagate into that inhomogeneity because it will shrink as long as the background is matter dominated. Even if the condition that the bubble nucleates comovingly is relaxed, such that the bubble may have $\partial_t \bar{r}(t_0) > 0$, deceleration is large enough to make the bubble contract almost immediately. Therefore it seems that studying the effect of curvature inhomogeneity within this approach is hardly feasible. Note that this result appears to be in contrast to what has been obtained in [29].

Nevertheless, to see what happens when a bubble enters a curvature inhomogeneity

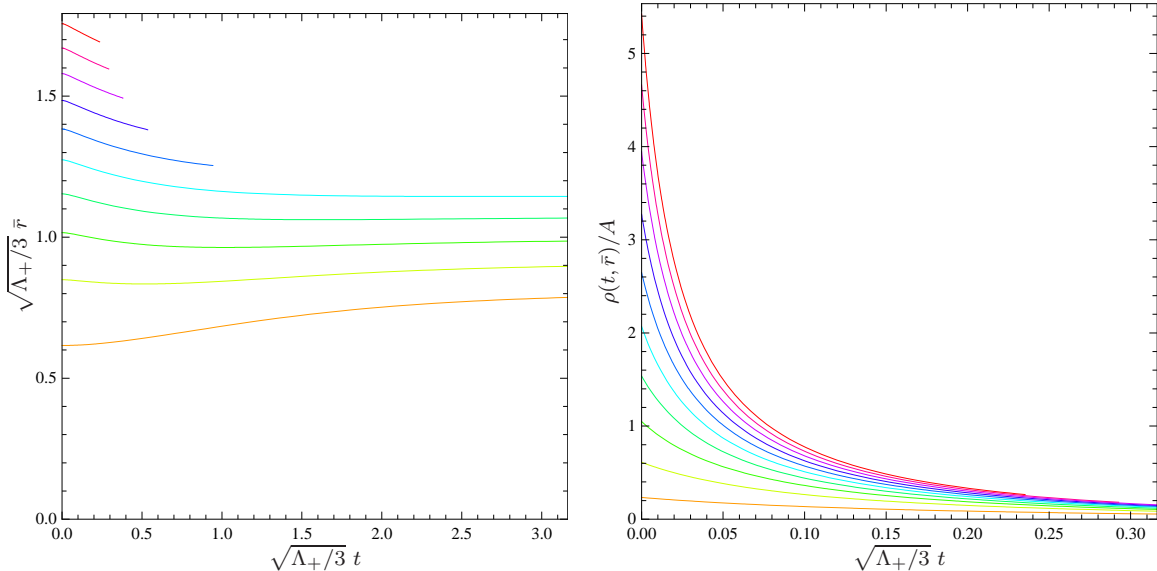


Figure 6. Results obtained for the inhomogeneous LTB model with the dust profile (55). The left figure shows the trajectory of bubbles with initial surface tension $0.7\sqrt{\Lambda_+/3} \leq 4\pi\sigma_0 \leq 1.6\sqrt{\Lambda_+/3}$ and $\Lambda_- = 0.1\Lambda_+$. Smaller bubbles nucleate in a region where vacuum energy dominates over dust density and therefore expand. Bubbles with $\bar{r}_0 \simeq r_A$ contract because they are already in a dust dominated background. The right figure shows the dust density at the position of the bubble. Although the dust profile (55) radially increases, the expansion of the background dilutes matter efficiently such that expanding bubbles effectively propagate in a decreasing profile.

we make use of a result obtained previously. In the last section it was shown that bubbles which nucleated in a vacuum dominated region expanded initially. Now, we add some curvature in ‘front’ of the bubble and have a look what happens if the bubble encounters that inhomogeneity and whether there is a difference compared to the corresponding solution in the flat background. The curvature profile is given by

$$k(r) = \frac{1}{2(\alpha_1 \mathcal{R}_{\text{cr}})^2} \left(1 + \tanh \left(\frac{\sqrt{\Lambda_+/3} r - \alpha_3}{\alpha_2} \right) \right), \quad (56)$$

where $\mathcal{R}_{\text{cr}} \equiv (4\pi A \sqrt{\Lambda_+})^{-1/3}$. Taking the dust profile from the last section, we fix the initial surface tension and vacuum energy of the bubble to $\sigma_0 = 0.6\sqrt{\Lambda_+/3}$, $\Lambda_- = 0.1\Lambda_+$. The evolution of the bubble is significantly affected in the exterior perspective. However, this may be just a coordinate effect and when looked at the trajectories in the interior coordinates the effect practically vanishes. Nevertheless, there remains an effect in the surface tension of the bubble, see Fig. 7.

3.3.3. Numerical solution in de Sitter/FLRW spacetime In this section, the evolution of the bubble on a de Sitter/FLRW background will be considered. The FLRW part is supposed to contain vacuum energy and a perfect fluid which undergoes a phase transition i) from $w = 1/3$ to $w = -1$, or ii) vice versa. The FLRW dynamics (28)

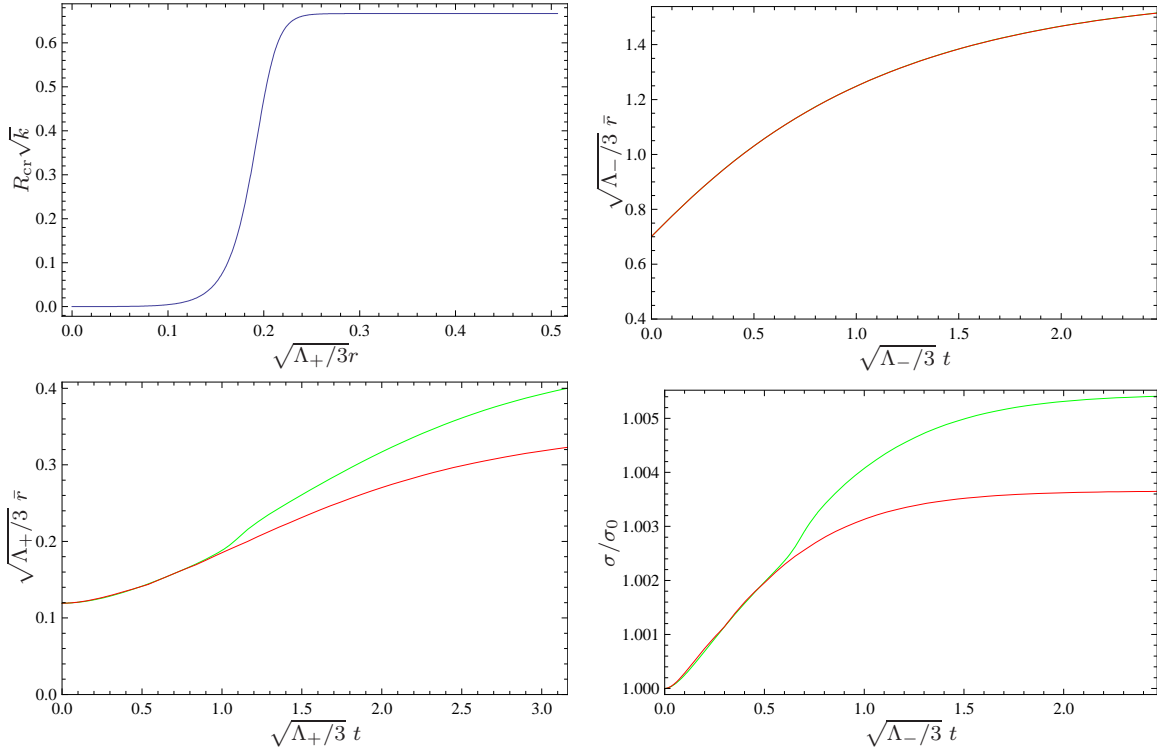


Figure 7. Results obtained for a bubble propagating in an inhomogeneous background (curvature inhomogeneity *and* inhomogeneity in the initial dust profile). Upper left: the curvature profile (56) with $\alpha_1 = 1.5, \alpha_2 = 0.02$ and $\alpha_3 = 0.2$. Lower left: Bubble trajectories in the comoving LTB coordinates in a flat background (red) compared to the curved background (green). The trajectories are affected significantly in these coordinates. However, if one converts the trajectories to the interior de Sitter coordinates the effect practically vanishes (upper right). Nevertheless, there remains an effect on the surface tension of the bubble (lower right).

and (29) will be solved numerically with the initial values $a(t_0) = 1$, $8\pi\rho_0/3 = 10^{-4}$ and $\Lambda_+/3 = 10^{-5}$. Again $t_0 = 0$ shall represent the exterior time coordinate at which $\partial_t\bar{r}(t_0) = 0$. The phase transition is supposed to occur at $t_{\text{pt}} = 0.5H_0^{-1}$, and we set the width $\gamma_{\text{pt}}^{-1} = 1 \ll H_0^{-1}$ in order to model a nearly instantaneous transition. After these dynamics have been established we consider the evolution of the bubble.

The nucleation radius of the bubble can still be obtained from equation (52) with $k = 0$. Of course, an immediate effect of the phase transition on the trajectory of the bubble can be seen in the exterior coordinates. In case i) the contraction of the bubble is stopped when the background becomes vacuum dominated, whereas in case ii) the expansion of the bubble reverses to contraction due to the phase transition. However, contrary to the inhomogeneous background discussed before, the effect is still present when the trajectory is expressed in the coordinates of an interior observer, see Fig. 8. However, the most prominent effect still can be seen in the surface tension of the bubble.

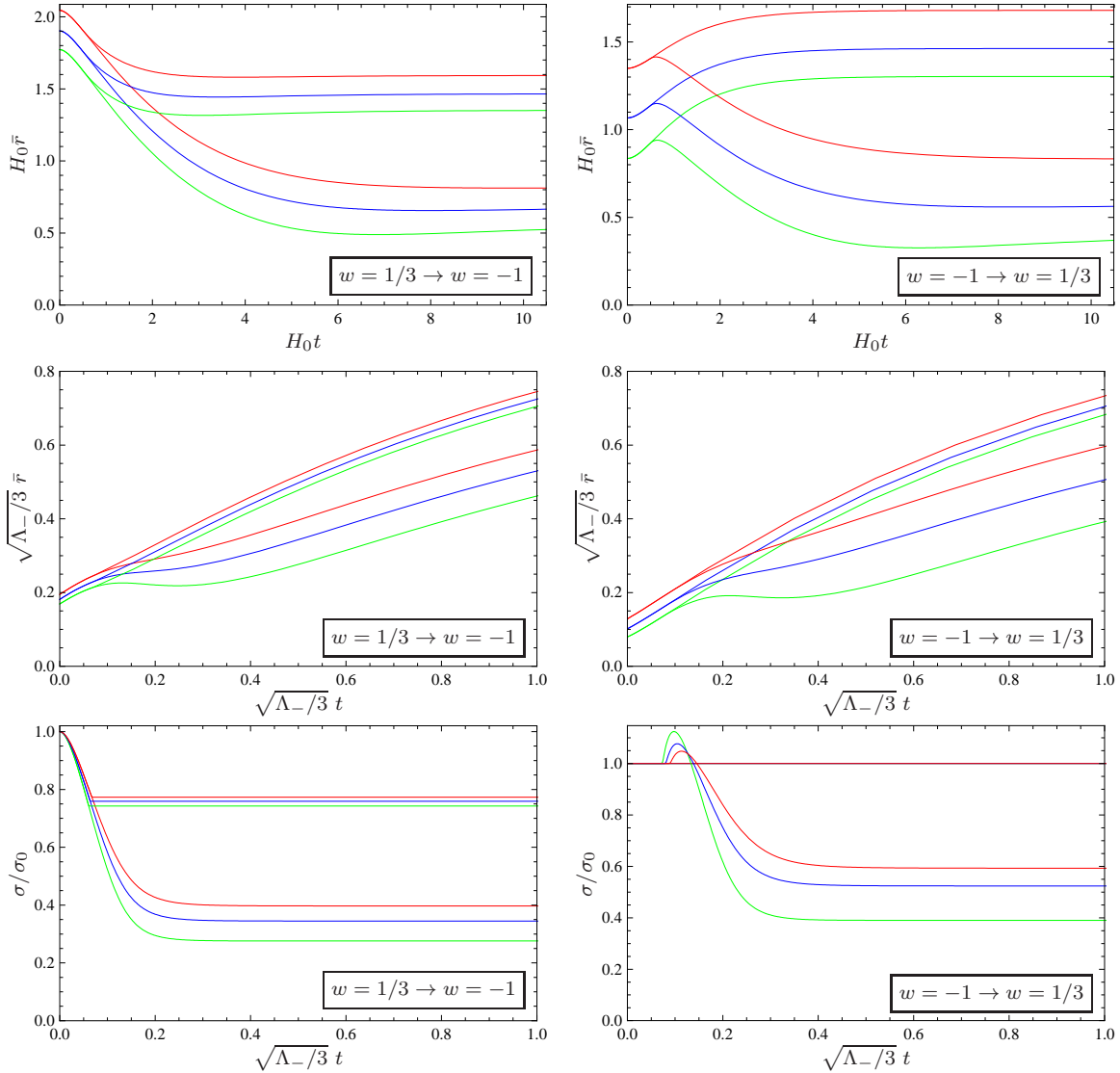


Figure 8. Evolution of bubbles in the de Sitter/FLRW spacetime for surface tensions $0.4H_0 \leq 4\pi\sigma \leq 0.6H_0$ and $\Lambda_- = 0.1\Lambda_+$. The left column shows the results of a transition from $w = 1/3$ to $w = -1$ and the right column from $w = -1$ to $w = 1/3$ compared, respectively, to their counterparts where the equation of state remains constant. The upper plots show the trajectory of the bubble in exterior coordinates, while the mid plots show the trajectories as seen from an interior observer. Unlike for the inhomogeneous background, we see that the exterior phase transition indeed leaves a sizeable effect on the trajectory of the bubble. In addition, the most prominent effect is again on the surface tension.

4. Conclusions

First-order phase transitions, as may have occurred multiple times in the early universe, proceed by spontaneous nucleation of bubbles. In order to answer the question on how much information about the initial state ‘survives’ the phase transition, it is important to understand bubble nucleation and propagation beyond the assumption of a trivial initial state. This question may indeed be relevant for certain cosmological scenarios, such as the chain inflation proposal. In this particular scenario, a series of first-order phase transitions proceeds very quickly, such that the time in between two transitions is too short for the universe to dilute all inhomogeneities and thermal radiation produced in each transition.

We have seen that the dynamics of the background spacetime affects the calculation of semiclassical tunneling probabilities. A simple comparison of time scales helps to decide if this effect is relevant. In cases where the bubble crossing time (the nucleation radius of the bubble divided by the speed of light) is much smaller than any time scale of the background geometry, we found that it is well justified to use tunneling rates obtained from field theory on Minkowski spacetime. Noting that this tunneling probability drops exponentially with increasing nucleation radius, it seems reasonable to assume that the bubbles in fact nucleate at tiny radii whenever we demand an appreciable tunneling rate which can lead to an onset of the phase transition before the universe reaches (approximately) a vacuum state. Hence, using Minkowski spacetime as an approximation appears self-consistent in many cases. However, if the expansion rate of the universe is very large, there may be cases where the effect of background evolution on tunneling rates can be important. In the context of the chain inflation proposal, we expect this to be the case very early on during a radiation dominated phase short after a previous phase transition.

The existence of a particle horizon in a radiation dominated FLRW universe renders the nucleation of bubbles larger than this horizon impossible. This means that one has to have better knowledge of the spacetime near the singularity, including details about reheating and any cosmology preceding the radiation era, in order to avoid this ‘horizon problem’. In other words, the pure radiation dominated FLRW universe is no useful approximation for a semiclassical calculation of nucleation rates of bubbles larger than the particle horizon, since those rates would be sensitive to the cosmology at the Big Bang.

Concerning the subsequent evolution of comovingly nucleated vacuum bubbles in non-vacuum backgrounds, we have seen that already the presence of homogeneously distributed matter has a significant influence on the bubble. Unlike in de Sitter spacetime where the proper kinetic energy of a bubble increases exponentially, it may decrease in the presence of matter in the background. For small bubbles, the proper kinetic energy became zero and real classical solutions could not be obtained beyond this point. As has been pointed out in [29], such bubbles do not correspond to classical configurations, but should be interpreted as mere fluctuations. Bubbles with greater

radius have more proper kinetic energy and are able to survive until the matter density in the background has been diluted sufficiently. We note, however, that the setup in which we study bubble trajectories, in particular the choice of initial conditions, is somewhat ad hoc. To settle this issue, one would have to solve the tunneling problem with matter *and* gravity, an enterprise on which we did not embark in this work.

We also studied the effect of inhomogeneities in the background on the propagation of vacuum bubbles. The results show that the trajectory of a bubble is affected, from the point of view of an exterior observer, when it propagates into an inhomogeneous background. Since it is not clear whether this is just a coordinate effect we have looked at the trajectory as seen by an interior observer. This observer will hardly see an influence of ambient inhomogeneities in the trajectory of the bubble. Nevertheless, when looked at from the inside, there remains an effect on the surface tension of the bubble.

Furthermore, bubbles moving in an FLRW spacetime which itself undergoes a phase transition have been considered. Similar to the inhomogeneous case, a large effect is seen in the exterior coordinates. However, when converted to interior coordinates, there remains an appreciable effect in the trajectory of the bubble. This raises the question whether those perturbations of the bubble wall will lead to potentially observable effects. In the context of bubble collisions [53, 54], it has been pointed out that a disturbance in the trajectory of the bubble wall may lead to a redshift of the reheating surface and could therefore potentially be observable in the CMB.

However, the most prominent of the effects of inhomogeneity or phase transitions in the background is found in the surface tension of the bubble. This is a consequence of the spacetime junction approach. As soon as a bubble propagates in a matter environment the evolution of its surface tension is determined by the demand of the background. This means that an expanding bubble ‘collects’ matter from the background while a contracting bubble will lose the amount of energy required by the space it uncovers. Therefore it is necessary to find a proper treatment of energy transfer through the bubble surface. Rather than fixing interior and exterior spacetime ab initio, one should dynamically construct those spacetimes from initial conditions. To solve this problem, an additional equation is needed, which arises from a proper dynamical description of the surface tension. It should capture the physics of matter transfer across the junction hypersurface and should probably be motivated from a field theoretical point of view. We hope to make progress in this direction in our future work.

Acknowledgments

We thank Ben Freivogel, I-Sheng Yang, Anthony Aguirre, and Douglas Spolyar for helpful discussions and suggestions. This work was supported by the German Research Foundation (DFG) through the Research Training Group 1147 ‘Theoretical Astrophysics and Particle Physics’.

Appendix A: Evolution equations in de Sitter/FLRW spacetime

For the proposed FLRW spacetime the relevant equations can be obtained in the same way as for the LTB part by setting $\partial_r a = 0$ and $E = 0$.

$$ar = R, \quad \dot{t}^2 = 1 + a^2 \dot{r}^2. \quad (\text{A.1})$$

The potential V reduces to

$$2V = - \left[\frac{\Lambda_-}{3} + \left(\frac{\rho}{3\sigma} + \frac{\Lambda_+ - \Lambda_-}{24\pi\sigma} + 2\pi\sigma \right)^2 \right] R^2, \quad (\text{A.2})$$

and the equations of motion are given by

$$\partial_t \bar{r} = \frac{\bar{r} \partial_t a - \sqrt{(1 + 2V) ((\bar{r} \partial_t a)^2 + 2V)}}{2aV}, \quad (\text{A.3})$$

$$\partial_t \sigma = (\rho + p) \frac{a \partial_t \bar{r}}{\sqrt{1 - (a \partial_t \bar{r})^2}}. \quad (\text{A.4})$$

These equations together with the background dynamics given by (28) and (29) determine the bubble motion in the de Sitter/FLRW background.

Bibliography

- [1] A. H. Guth, *Inflation and eternal inflation*, *Phys. Rept.* **333** (2000) 555, [[arXiv:astro-ph/0002156](#)], [[NASA-ADS](#)], [[SPIRES](#)].
- [2] A. Linde, *Inflationary cosmology*, *Lect. Notes Phys.* **738** (2008) 1–54, [[arXiv:0705.0164](#)], [[NASA-ADS](#)], [[SPIRES](#)].
- [3] L. McAllister and E. Silverstein, *String cosmology: a review*, *Gen. Rel. Grav.* **40** (2008) 565, [[arXiv:0710.2951 \[hep-th\]](#)], [[NASA-ADS](#)], [[SPIRES](#)].
- [4] L. Susskind, *The anthropic landscape of string theory*, [[arXiv:hep-th/0302219](#)], [[NASA-ADS](#)], [[SPIRES](#)].
- [5] M. R. Douglas and S. Kachru, *Flux compactification*, *Rev. Mod. Phys.* **79** (2007) 733, [[arXiv:hep-th/0610102](#)], [[NASA-ADS](#)], [[SPIRES](#)].
- [6] S. R. Coleman and F. De Luccia, *Gravitational effects on and of vacuum decay*, *Phys. Rev. D* **21** (1980) 3305, [[NASA-ADS](#)], [[SPIRES](#)].
- [7] S. W. Hawking and I. G. Moss, *Supercooled phase transitions in the very early universe*, *Phys. Lett. B* **110** (1982) 35 [[NASA-ADS](#)], [[SPIRES](#)].
- [8] J. Garriga, D. Schwartz-Perlov, A. Vilenkin and S. Winitzki, *Probabilities in the inflationary multiverse*, *JCAP* **0601** (2005) 017, [[arXiv:hep-th/0509184](#)], [[NASA-ADS](#)], [[SPIRES](#)].
- [9] S. R. Coleman, *The fate of the false vacuum. 1. Semiclassical theory*, *Phys. Rev. D* **15** (1977) 2929, Erratum-ibid. *D* **16** (1977) 1248, [[NASA-ADS](#)], [[SPIRES](#)], [[KEK](#)].
- [10] K. Freese and D. Spolyar, *Chain inflation: 'Bubble bubble toil and trouble'*, *JCAP* **0507** (2005) 007, [[arXiv:hep-ph/0412145](#)], [[NASA-ADS](#)], [[SPIRES](#)].
- [11] S. Watson, M. J. Perry, G. L. Kane and F. C. Adams, *Inflation without inflaton(s)*, *JCAP* **0711** (2007) 017 [[arXiv:hep-th/0610054](#)], [[NASA-ADS](#)], [[SPIRES](#)].
- [12] B. Feldstein and B. Tweedie, *Density perturbations in chain inflation*, *JCAP* **0704** (2007) 020, [[arXiv:hep-ph/0611286](#)], [[NASA-ADS](#)], [[SPIRES](#)].
- [13] K. Freese, J. T. Liu and D. Spolyar, *Chain inflation via rapid tunneling in the landscape*, [[arXiv:hep-th/0612056](#)], [[NASA-ADS](#)], [[SPIRES](#)].

- [14] Q. G. Huang, *Simplified chain inflation*, *JCAP* **0705** (2007) 009, [[arXiv:0704.2835 \[hep-th\]](#)], [[NASA-ADS](#)], [[SPIRES](#)].
- [15] D. Chialva and U. H. Danielsson, *Chain inflation revisited*, *JCAP* **0810** (2008) 012, [[arXiv:0804.2846 \[hep-th\]](#)], [[NASA-ADS](#)], [[SPIRES](#)].
- [16] D. Chialva and U. H. Danielsson, *Chain inflation and the imprint of fundamental physics in the CMBR*, *JCAP* **0903** (2009) 007, [[arXiv:0809.2707 \[hep-th\]](#)], [[NASA-ADS](#)], [[SPIRES](#)].
- [17] A. Ashoorioon, K. Freese and J. T. Liu, *Slow nucleation rates in chain inflation with QCD axions or monodromy*, *Phys. Rev. D* **79** (2009) 067302, [[arXiv:0810.0228 \[hep-ph\]](#)], [[NASA-ADS](#)], [[SPIRES](#)].
- [18] A. Ashoorioon and K. Freese, *Gravity waves from chain inflation*, [[arXiv:0811.2401 \[hep-th\]](#)], [[NASA-ADS](#)], [[SPIRES](#)].
- [19] S. Sarangi, G. Shiu and B. Shlaer, *Rapid tunneling and percolation in the landscape*, *Int. J. Mod. Phys. A* **24** (2009) 741, [[arXiv:0708.4375 \[hep-th\]](#)], [[NASA-ADS](#)], [[SPIRES](#)].
- [20] S.-H. H. Tye, *A new view of the cosmic landscape*, [[arXiv:hep-th/0611148](#)], [[NASA-ADS](#)], [[SPIRES](#)].
- [21] R. M. Wald, *Asymptotic behavior of homogeneous cosmological models in the presence of a positive cosmological constant*, *Phys. Rev. D* **28** (1983) 2118, [[NASA-ADS](#)], [[SPIRES](#)].
- [22] L. G. Jensen and J. A. Stein-Schabes, *Is inflation natural?*, *Phys. Rev. D* **35** (1987) 1146, [[NASA-ADS](#)], [[SPIRES](#)].
- [23] Y. Kitada and K.-i. Maeda, *Cosmic no hair theorem in homogeneous space-times. 1. Bianchi models*, *Class. Quant. Grav.* **10** (1993) 703, [[NASA-ADS](#)], [[SPIRES](#)].
- [24] M. A. S. Nobre, M. R. d. Maia, J. C. Carvalho and J. A. S. Lima, *Inhomogeneous inflation and cosmic no-hair conjecture*, [[arXiv:0903.3449 \[gr-qc\]](#)], [[NASA-ADS](#)], [[SPIRES](#)].
- [25] G. W. Gibbons and S. W. Hawking, *Cosmological event horizons, thermodynamics, and particle creation*, *Phys. Rev. D* **15** (1977) 2738 [[NASA-ADS](#)], [[SPIRES](#)].
- [26] A. A. Starobinski, *Isotropization of arbitrary cosmological expansion given an effective cosmological constant*, *Piz'ma Zh. Eksp. Teor. Fiz.* **37** (1983) 55, [[NASA-ADS](#)].
- [27] P. M. Saffin, A. Padilla and E. J. Copeland, *Decay of an inhomogeneous state via resonant tunnelling*, *JHEP* **0809** (2008) 055, [[arXiv:0804.3801 \[hep-th\]](#)], [[NASA-ADS](#)], [[SPIRES](#)].
- [28] E. J. Copeland, A. Padilla and P. M. Saffin, *No resonant tunneling in standard scalar quantum field theory*, *JHEP* **0801** (2008) 066, [[arXiv:0709.0261 \[hep-th\]](#)], [[NASA-ADS](#)], [[SPIRES](#)].
- [29] W. Fischler, S. Paban, M. Žanić and C. Krishnan, *Vacuum bubble in an inhomogeneous cosmology: a toy model*, *JHEP* **0805** (2008) 041, [[arXiv:0711.3417 \[hep-th\]](#)], [[NASA-ADS](#)], [[SPIRES](#)].
- [30] D. S. Goldwirth and T. Piran, *Initial conditions for inflation*, *Phys. Rept.* **214** (1992) 223, [[NASA-ADS](#)], [[SPIRES](#)].
- [31] E. Calzetta and M. Sakellariadou, *Inflation in inhomogeneous cosmology*, *Phys. Rev. D* **45** (1992) 2802 [[NASA-ADS](#)], [[SPIRES](#)].
- [32] H. Kurki-Suonio, P. Laguna and R. A. Matzner, *Inhomogeneous inflation: numerical evolution*, *Phys. Rev. D* **48** (1993) 3611, [[arXiv:astro-ph/9306009](#)], [[NASA-ADS](#)], [[SPIRES](#)].
- [33] N. Deruelle and D. S. Goldwirth, *Conditions for inflation in an initially inhomogeneous universe*, *Phys. Rev. D* **51** (1995) 1563, [[arXiv:gr-qc/9409056](#)], [[NASA-ADS](#)], [[SPIRES](#)].
- [34] O. Iguchi and H. Ishihara, *Onset of inflation in inhomogeneous cosmology*, *Phys. Rev. D* **56** (1997) 3216, [[arXiv:gr-qc/9611047](#)], [[NASA-ADS](#)], [[SPIRES](#)].
- [35] A. Berera and C. Gordon, *Inflationary initial conditions consistent with causality*, *Phys. Rev. D* **63** (2001) 063505, [[arXiv:hep-ph/0010280](#)], [[NASA-ADS](#)], [[SPIRES](#)].
- [36] C. W. Misner, K. S. Thorne and J. A. Wheeler, *Gravitation*, 1279 pp., W. H. Freeman, San Francisco (1973), [[NASA-ADS](#)], [[SPIRES](#)].
- [37] W. Fischler, D. Morgan and J. Polchinski, *Quantization of false-vacuum bubbles: A Hamiltonian treatment of gravitational tunneling*, *Phys. Rev. D* **42** (1990) 4042, [[NASA-ADS](#)], [[SPIRES](#)].
- [38] L. M. Widrow, *False-vacuum decay in time-dependent and two-field models*, *Phys. Rev. D* **44** (1991) 2306, [[NASA-ADS](#)], [[SPIRES](#)].

- [39] E. Keski-Vakkuri and P. Kraus, *Tunneling in a time dependent setting*, [Phys. Rev. D **54** \(1996\) 7407](#), [[arXiv:hep-th/9604151](#)], [[NASA-ADS](#)], [[SPIRES](#)].
- [40] L. F. Abbott, D. Harari and Q.-H. Park, *Vacuum decay in curved backgrounds*, [Class. Quant. Grav. **4** \(1987\) L201](#), [[NASA-ADS](#)], [[SPIRES](#)].
- [41] R. Basu, A. H. Guth and A. Vilenkin, *Quantum creation of topological defects during inflation*, [Phys. Rev. D **44** \(1991\) 340](#), [[NASA-ADS](#)], [[SPIRES](#)], [[KEK](#)].
- [42] W. Israel, *Singular hypersurfaces and thin shells in general relativity*, [Nuovo Cim. **B44S10** \(1966\)1](#), Erratum-ibid. B **48** (1967 NUCIA,B44,1.1966) 463, [[NASA-ADS](#)].
- [43] G. A. Lemaître and M. A. H. MacCallum, *The expanding universe*, [Gen. Rel. Grav. **29** \(1997\) 641](#) [[Annales Soc. Sci. Brux. Ser. I Sci. Math. Astron. Phys. A **53** \(1933\) 51](#)], [[NASA-ADS](#)], [[SPIRES](#)].
- [44] R. Tolman, *Effect of inhomogeneity on cosmological models*, [Proc. Nat. Acad. Sci. **20** \(1934\) 169](#), [[NASA-ADS](#)].
- [45] H. Bondi. *Spherically symmetrical models in general relativity*, [Mon. Not. R. Astron. Soc. **107** \(1947\) 410](#) [[NASA-ADS](#)].
- [46] S. K. Blau, E. I. Guendelman and A. H. Guth, *Dynamics of false-vacuum bubbles*, [Phys. Rev. D **35** \(1987\) 1747](#), [[NASA-ADS](#)], [[SPIRES](#)], [[KEK](#)].
- [47] J. Plebański and A. Krasinski, *An introduction to general relativity and cosmology*, 534 pp., Cambridge, UK: Cambridge Univ. Pr. (2006), [[SPIRES](#)].
- [48] E. Poisson, *A relativist's toolkit: The mathematics of black-hole mechanics*, 250 pp., Cambridge, UK: Cambridge Univ. Pr. (2004), [[NASA-ADS](#)].
- [49] Ø. Grøn and S. Hervik, *Einsteins general theory of relativity*, 500 pp., Springer, Berlin (2007).
- [50] V. A. Berezin, V. A. Kuzmin and I. I. Tkachev, *Dynamics of bubbles in general relativity*, [Phys. Rev. D **36** \(1987\) 2919](#), [[NASA-ADS](#)], [[SPIRES](#)], [[KEK](#)].
- [51] A. Aurilia, M. Palmer and E. Spallucci, *Evolution of bubbles in a vacuum*, [Phys. Rev. D **40** \(1989\) 2511](#), [[NASA-ADS](#)], [[SPIRES](#)], [[KEK](#)].
- [52] A. Aguirre, M. C. Johnson, *Dynamics and instability of false vacuum bubbles*, [Phys. Rev. D **72** \(2005\) 10525](#), [[arXiv:gr-qc/0508093](#)], [[NASA-ADS](#)], [[SPIRES](#)].
- [53] A. Aguirre, M. C. Johnson and M. Tysanner, *Surviving the crash: assessing the aftermath of cosmic bubble collisions*, [Phys. Rev. D **79** \(2009\) 123514](#), [[arXiv:0811.0866 \[hep-th\]](#)], [[NASA-ADS](#)], [[SPIRES](#)].
- [54] S. Chang, M. Kleban and T. S. Levi, *Watching worlds collide: effects on the CMB from cosmological bubble collisions*, [JCAP **0904** \(2009\) 025](#), [[arXiv:0810.5128 \[hep-th\]](#)], [[NASA-ADS](#)], [[SPIRES](#)].